Among carbon-based nanomaterials, activated carbon, carbon nanotubes (B. Yu et al. 2015), mesoporous carbon, graphene [Zhang et al. (2015), Khare et al. (2013), Zeng et al. (2018) Gusain et al. (2016), Gupta et al. (2016), Peng et al. (2015), Ye et al. (2016)], fullerenes [Lee et al. (2007)], carbon spheres [Alazemi et al. (2015), Song et al. (2018)], carbon nano-onions [Joly-Pottuz et al. (2008)], and alike have been extensively studied as lubrication additives, specifically for reducing friction and wear. Their spherical structure is an advantage over other forms, especially in lubrication as it makes them ideal rolling bearings during lubrication, which keep the tribo-pairs far apart and mitigate friction and wear. Ultrasmooth sub-micrometre carbon spheres have been prepared by polymerization of formaldehyde and resorcinol under ultrasound and then using heat treatment. These carbon spheres were found to be efficient antiwear and antifriction additives. Carbon spheres undoubtedly are very important in lubrication, but under extreme conditions, their rolling action is restricted due to their contorted shape [Alazemi et al. (2015)]. The rubbing waste may further add undue friction. Reinforcement of carbon spheres by polyimide polymer or silver nanoparticles has yielded very good triboactivity [Song et al. (2018)]. Thus, the hybrid materials having characteristics of both the constituents naturally draw more preference over the individual ones.

In addition to this, carbon spheres have been acknowledged for their multifarious activities like drug delivery [Yang et al. (2013)], bio-diagnostics [Ray et al. (2009)], photonic bandgap crystals [Sun et al. (2004), Pei et al. (2016)], supercapacitor [Lui et al. (2015), Wickramaratne et al. (2013), Jia et al. (2015) and lubrication [Alazemi et al. (2015)]. Noble metal nanoparticles of copper, silver, gold, palladium and platinum

have been placed on or encapsulated in carbon spheres for catalytic [De et al. (2017)], magnetic, electronic or optoelectronic [Yang et al. (2013)] applications.

Besides anti-bacterial [Yun et al. (2012), Chatterjee et al. (2014)], anti-microbial [Ramyadevi et al. (2012), Delgado et al. (2011)] and anti-fungal applications, copper nanoparticles are equally important as high strength metals/ alloys, thermal conductive materials [Wang et al. (2012)], efficient catalysts [Reske et al. (2014), Guo et al. (2014)] and nanometal lubricant additives [Zhou et al. (2000), Kreivaitis et al. (2013)]. It appeared us as the most enthralling to prepare carbon spheres and fabricate a hybrid incorporating copper nanoparticles for synergistic furtherance of triboactivity even at very high loads. Enhanced dispersibility of the hybrids in the lubricating oil compared to just nanoparticles, further favours their application as antiwear and antifriction additives.

In the present chapter, carbon spheres, copper nanoparticles and their composite have been synthesized hydrothermally and evaluated for their tribo-activity in paraffin base lube on a four-ball tester.

5.1. Materials & methods

5.1.1. Chemicals

The chemicals used in this work, glucose, ascorbic acid, copper acetate trihydrate and citric acid were AR grade and used without further purification.

5.1.2. Synthesis of additives

5.1.2.1. Preparation of carbon spheres (C)

In the present work, carbon spheres were synthesized by carbonization of glucose and ascorbic acid using a one-step hydrothermal method [De et al. (2017)]. In this procedure, homogeneous aqueous solutions of glucose (0.5 M) and ascorbic acid (0.1M) were prepared one by one in distilled water (30 mL) for each by sonication for1 h. The solution was poured into a 250 mL Teflon autoclave and was maintained at 180 ^{o}C for 12 h. The reaction product was cooled to room temperature and collected via centrifugation. It was washed several times with distilled water followed by ethanol. The product was dispersed again in absolute ethanol and sonicated for 1 h. The ethanol was evaporated, and the final product was dried in an oven.

5.1.2.2. Preparation of copper nanoparticles

Synthesis of copper nanoparticles was also accomplished by the hydrothermal method. In this method, aqueous solutions of copper acetate trihydrate (10 mmol) and citric acid (10 mmol) were prepared separately in 20 mL of distilled water for each, and the solution mixture was sonicated for 1 h. After sonication, the solution was transferred into 250 ml Teflon autoclave and maintained at temperature 180^{o}C for 12 h. The resulting product was cooled to room temperature and constantly washed with water and then ethanol via centrifugation. It was dispersed in ethanol followed by 1h sonication. The ethanol was evaporated until a dry product is obtained.

5.1.2.3. Preparation of Cu@C

Cu@C nanocomposite was also synthesized by the hydrothermal method [De et al. (2017)]. For a typical synthesis, 0.5 mole glucose and 0.1 mole ascorbic acid were dissolved in 25 mL of distilled water separately and mixed to form a uniform solution with the help of ultrasonication. Then, 10 mL $Cu(OAc)_2$ (0.2M) was added drop-wise into the above solution under incessant magnetic stirring for10 min. It was stirred further for 30 min after adding citric acid (0.4 mole) in 25 mL distilled water. The reaction mixture was transferred into a 250 mL Teflon autoclave and maintained at temperature 180^{o}C for 12 h. After the completion of the reaction, the product obtained was cooled to room temperature. It was washed over and over again with distilled water and then ethanol using centrifugation. The obtained Cu@C precipitate was dispersed in absolute ethanol and evaporated to dryness.

5.1.3. Sample preparation

The admixtures of paraffin oil with different additives carbon spheres/ Cu nanoparticles/ Cu@C were prepared in concentrations 0.05, 0.10, 0.15 0.20 (% w/v) by constant stirring at 40-50 $^{\circ}$C till 1h and subsequent sonication for 1h around 25 ^{o}C. The entire testing was carried out at an optimized additive concentration, 0.1 % w/v.

5.2. Results and discussion

5.2.1. Structural and morphological characteristics of the additives

The copper nanoparticles, carbon spheres and Cu@C spheres synthesized by environment-friendly methods have been characterized by FE-SEM, TEM/HR-TEM, XRD and XPS techniques.

The FE-SEM images of copper nanoparticles and Cu@C nanospheres are illustrated in **Fig. 5.1a and 5.1b**, respectively. **Fig. 5.1a** reveals the spherical shape of nanoparticles, while **Fig. 5.1b** presents nanoparticles placed on carbon nanospheres, having a size of approximately 100 nm. In **Fig. 5.1c** as per particle size distribution graph, around 70% particles are in the range 50 to 100 nm while approximately 30% lies in the range 100 to 150 nm and average particle size is clearly indicated as 100nm. The TEM images of the composite have also been taken for good discernment of morphology, and are displayed in **Fig. 5.2 a and b**. HR-TEM images show the spherical shape of nanoparticles and their size lies in the range 15-30 nm. Carbon spheres of size 80-115 nm are seen in the TEM images.

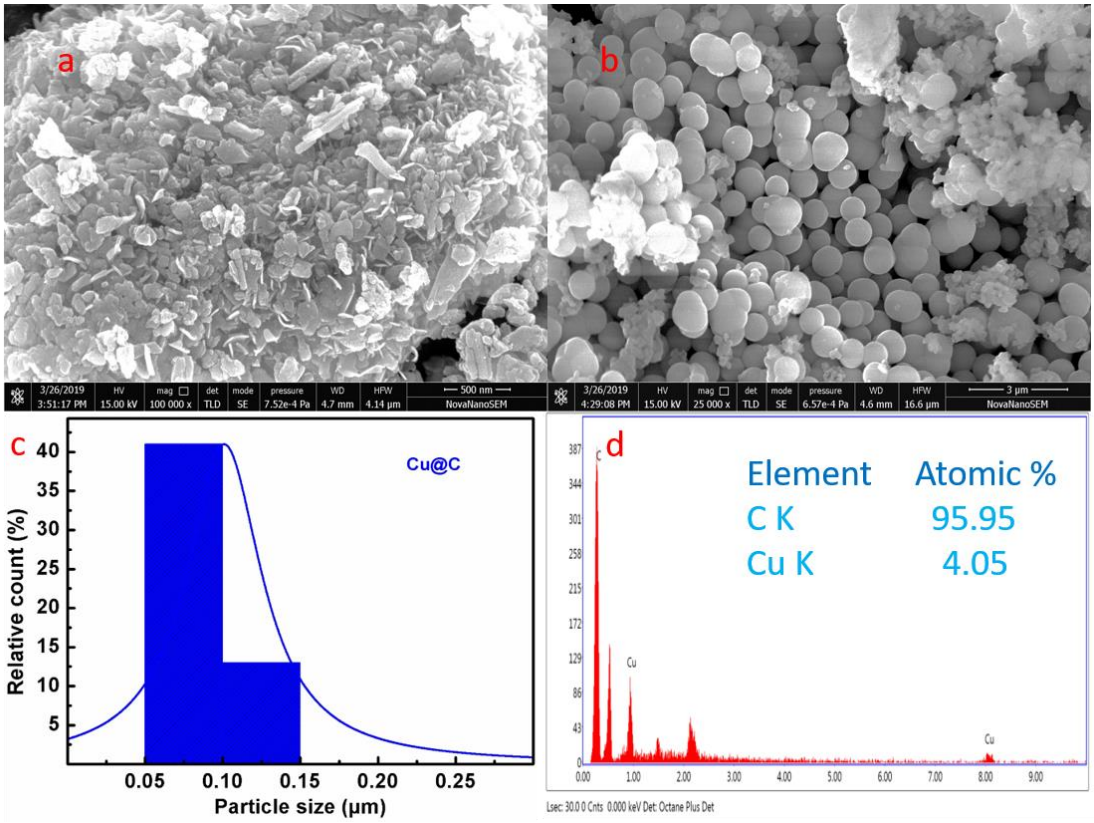

Fig. 5.1. FE-SEM images of (a) Cu (b) Cu@C, (c) Particle size distribution histogram of Cu@C and (d) EdX spectra of Cu@C

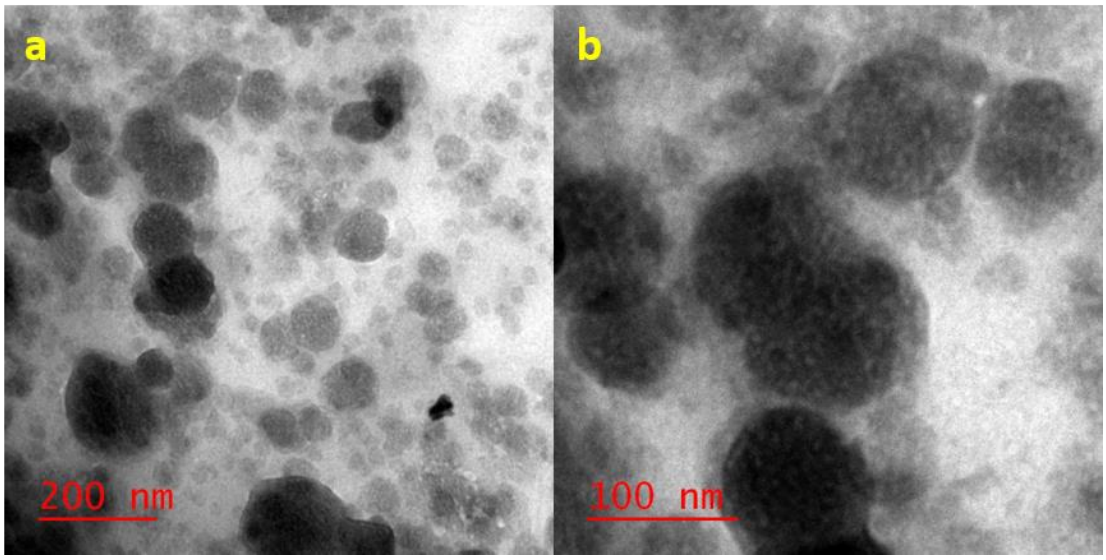

Fig. 5.2. TEM images of Cu@C composite at different magnification (a) 200 nm and (b) 100 nm

The EDX spectrum of the composite provides its elemental composition. The existence of evident signals due to copper and carbon together confirms that the suggested nanocomposite is formed. Furthermore, synthesis of Cu@C is accredited by atomic weight % data as given in **Fig. 5.1d.**

Fig. 5.3 shows X-ray diffraction (XRD) patterns of carbon spheres, copper nanoparticles and the composite Cu@C. Copper nanoparticles exhibit characteristic peaks at 43.3, 50.34 and 74.08^{o}corresponding to the (111), (200) and (220) planes respectively (JCPDS Card No. 08-0836) [Wang et al. (2012)] whereas in case of amorphous carbon only one wide peak is observed in the range 10–35^{o} (JCPDS 75-2078) [Song et al. (2018)]. However, the composite Cu@C shows the peaks due to copper and amorphous carbon at similar positions.

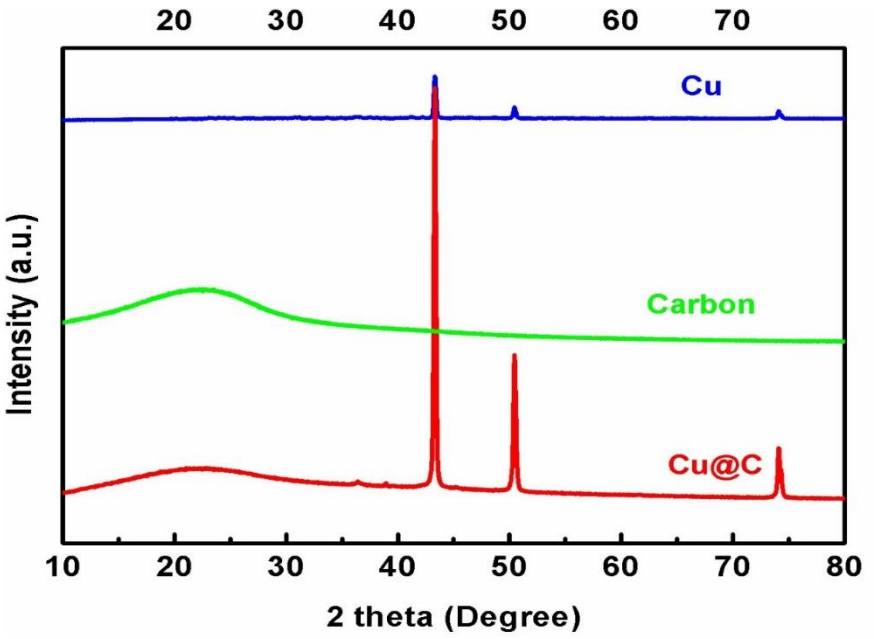

Fig. 5.3. XRD patterns of as-prepared Carbon spheres, Cu nanoparticle and Cu@C composite

As evident from the spectra, D and G bands are identified at 1371 and 1583 cm^{-1} [Song et al. (2018), Wang et al. (2009)]. The D band is ascribed to sp^3 carbon atoms while G band is allocated to in-plane vibrations of sp^2 graphitic carbon atoms. The I_D /I_G (proportional intensities) of these bands, is 0.78 for carbon spheres, which matches exactly with reported one suggesting disorderliness of the same level. The lower ratio of I_D /I_G for Cu@C, 0.71 is indicative of compatibility of copper nanoparticle with sp^2 arrangement of carbon atoms.

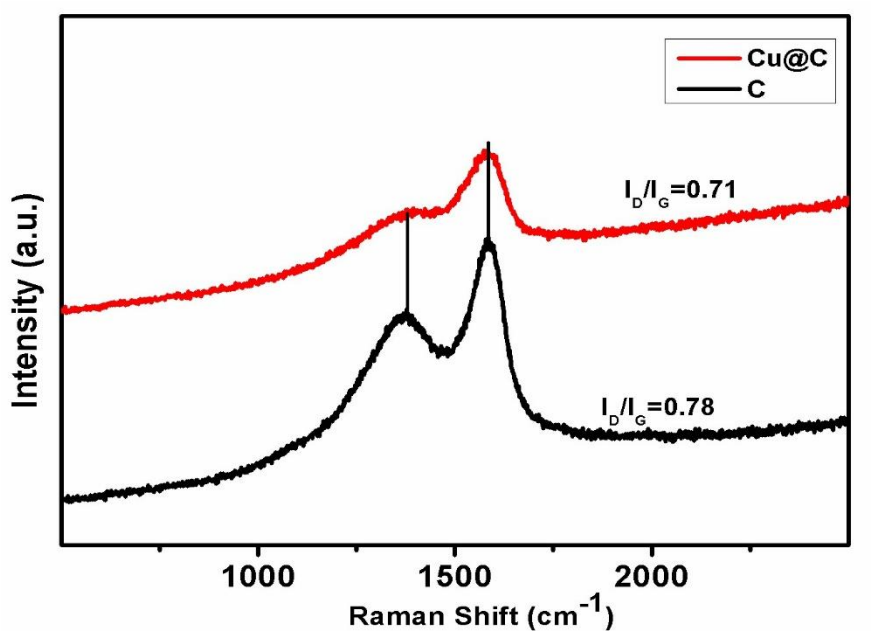

Fig. 5.4. Raman spectra of Carbon spheres and Cu@C composite

The chemical structure of composite Cu@C has been investigated by XPS studies. Deconvolution of the core level spectra with best-fitting parameters using peak fit software is displayed in **Fig. 5.5**. Thus, the core level spectra of C 1s yielded 4 peaks at 284.7, 285.5, 286.6and 288.4 eV binding energies corresponding to C-C, C-O, C=O and O-C=O bonds respectively, **Fig. 5.5a**. **Fig. 5.5b** describes Cu 2p core level spectrum showing two peaks with binding energies 932.1 and 952.4 eV attributed to Cu $2p_{3/2}$ and Cu $2p_{1/2}$ respectively. A relatively smaller peak observed at 940.8eV represents cupric ion in the paramagnetic state [De et al. (2017)].

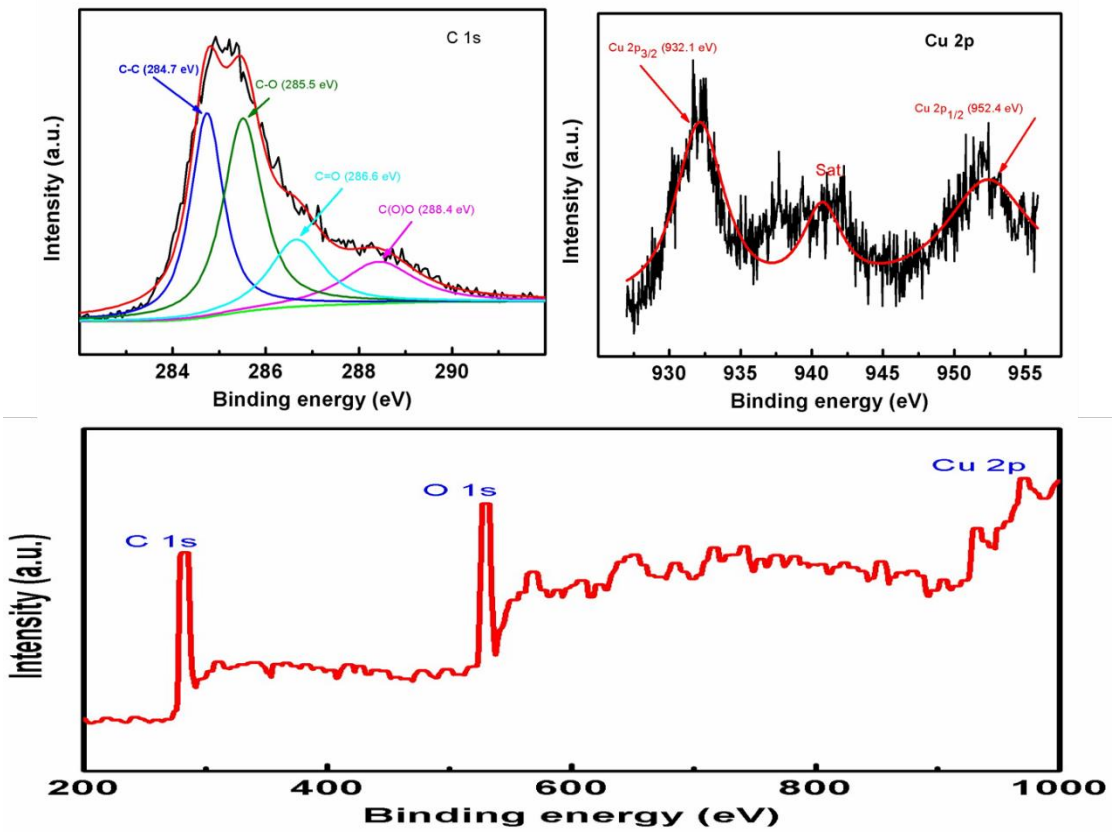

Fig. 5.5. Deconvoluted XPS images of Cu@C composite: C 1s core-level spectra, Cu 2p core-level spectra, and XPS survey spectra

5.2.2. Tribological properties

5.2.2.1. Dispersion stability of additives in paraffin oil

Dispersion stability of the studied additives was determined from the absorption data (in the region 200-800 nm) obtained from UV/visible spectroscopy after every 6 hours interval from zero to forty-eight hours. The optimized concentration of the admixtures was further 10 times diluted for recording the absorption values. The relative absorbance of all the admixtures against settling time has been plotted and shown in **Fig. 5.6a**. The relative absorbance in general decreases from zero to 48 h. A comparison of the additives shows that the relative absorbance with no shred of doubt

attenuates with time, but the attenuation is maximum with carbon and minimal with the composite. All the additives are, in fact, sufficiently stable as the attenuation in relative absorbance reaches up to 0.5 only that means there is around 50% reduction in absorbance within 48 h. The characteristics of absorbance for dispersion of Cu@C within 48 h at 6 h intervals are shown in the inset. The absorption band is visible at 254 nm, and its relative absorbance declines with time from 1 to 0.5 up to 48 h. **Fig. 5.6b** manifests the photographs of base oil and its dispersions with the composite initially and beyond 48 h.

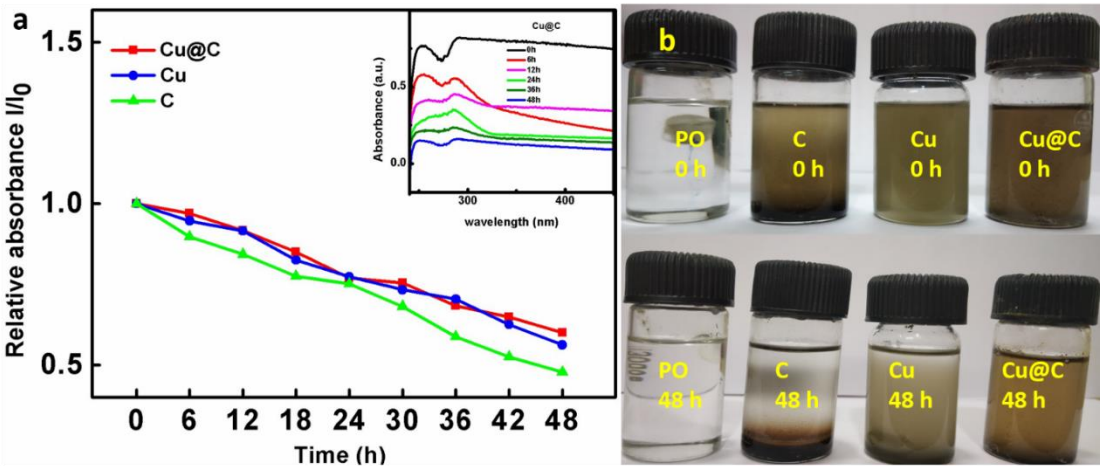

Fig. 5.6. (a) Dispersion stabilities of base oil containing Carbon Spheres, Cu nanoparticle and Cu@C composite studied by UV−vis spectrophotometry. (b) Optical photographs of different nano additives dispersed in base oil at different settling time

5.2.2.2. Additive optimization

The concentration of additives was optimized by measuring wear scar diameter (MWD) for different concentrations of additives in a base oil, 0.00, 0.05,0.10, 0.15 and 0.20% w/v at 392N load for 60 min run. **Fig. 5.7**, depicts how MWD varies with tested concentrations of the additives variation. The additives, in general, show tribological activity at all the concentrations. There is a remarkable decrease in MWD values for all the additives with an increase in concentration up to 0.10 %w/v. After that, a sudden increase in MWD is perceived in each case, which continues further for the next concentration, too. Thus, determinately 0.10 %w/v is the optimized concentration. It is distinctly visible from the figure that the composite shows the best activity throughout the tested concentrations followed by copper nanoparticles and at last the carbon spheres.

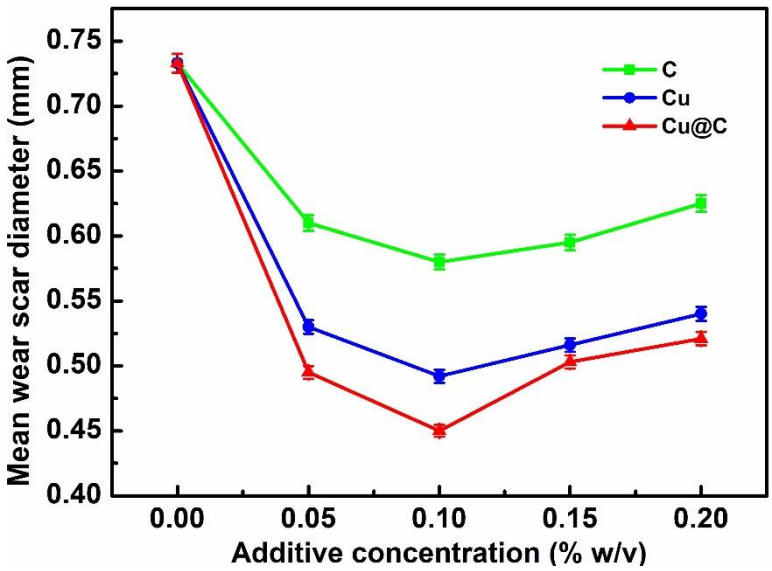

Fig. 5.7. Variation of mean wear scar diameter as a function of additive concentration (392 N, 60 min)

5.2.2.3 Antiwear and antifriction properties

The standard norms for ASTM D4172 test (392 load for 60 min.) were adopted to perform antiwear tests. The bar diagram, **Fig. 5.8**, presents the outcome of the tests focusing on MWD data and the average friction coefficient in paraffin oil and its formulations with different additives. It is observable from the figure that % reduction in MWD increases from carbon spheres (21) to Cu@C (38) through copper nanoparticles (33). Thus, a tremendous decrease in MWD values for the composite supports its outstanding tribological behaviour.

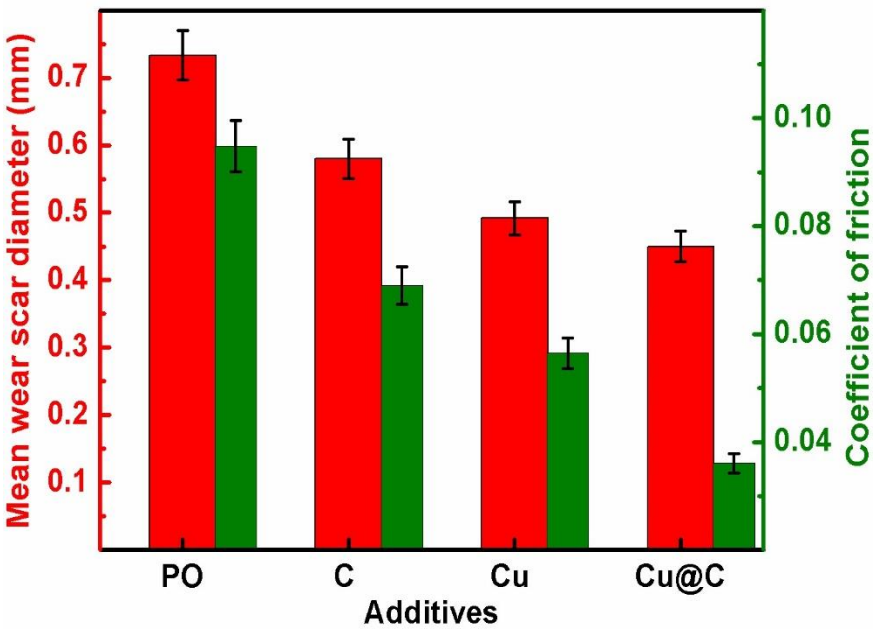

Fig. 5.8. Comparative analysis of wear scar diameter and coefficient of friction (COF) of different additives at an optimum concentration of 0.1% (w/v) in paraffin oil (392N, 60 min)

The average COF value 0.0948 for the base lube has also encountered a reduction in the tune similar to MWD, Carbon sphere (0.0691), copper nanoparticles (0.0564) and finally Cu@C (0.0360). The COF values follow the same trend as that observed for MWD data. Accordingly, the tested additives in general and Cu@C, in particular, appear to alter wear and friction significantly. The inherent characteristics of the tribochemical film formed during the test are categorically accountable for the observed activity. Carbon spheres and spherical nanoparticles both together have supported synergistically in the process of lubrication. Consequently, friction and wear are enormously reduced.

Fig. 5.9 shows plots of the friction coefficient (COF) versus sliding time at 392 N load in blank paraffin oil and its blends with the additives. It is a very important parameter from the viewpoint of life expectancy of machines. It is a general observation that the values of COF are high in the beginning. After some time when tribofilm formation starts, COF values invariably reduce in each case and at last get stabilised achieving a limiting value. As expected, COF values are the highest throughout the test for plain base oil but lowest for its blend with Cu@C. Such a low value of friction coefficient is anticipated to enhance the active life of machine parts.

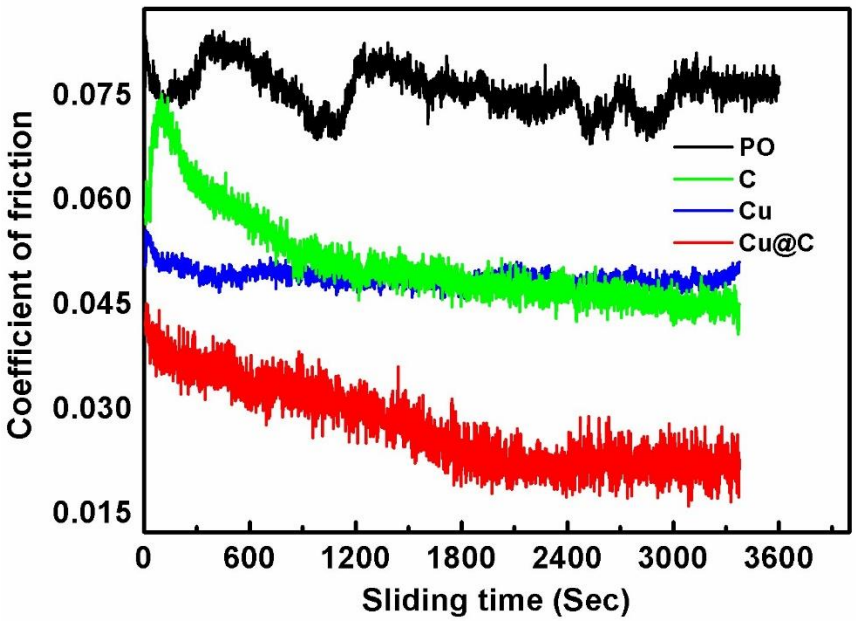

Fig. 5.9. Variation of the coefficient of friction with time (392 N, 1200 rpm, 3600 sec) for the studied additives in paraffin oil

5.2.2.3. Wear rate

In the next tribological test, MWD data has been recorded by changing time 0.25, 0.50, 0.75, 1, 1.25 and 1.5 h under the load of 392 N in base lube alone or accompanied with additives. From the observed MWD data, the corresponding mean wear volumes (MWV) have been calculated. **Fig. 5.10** Shows plots for MWV against sliding time. The linear regression model has been applied to find out the wear rate. It can be easily understood from the data in **Table 5.1** that both running-in and steady-state wear rates are much higher for plain oil. However, when additives are added, their values are dramatically attenuated. The reduction of wear rates exactly follows the order of antiwear efficacy of the studied additives. Steady-state wear rate, of course, is lesser than the running-in wear rate. For better life span, a tribo pair should

always have the lowest value for steady-state wear rate as far as possible. The composite Cu@C with the lowest value of steady-state rate manifests its applicability as a potential antiwear/antifriction additive. It may be pleaded authoritatively that both the Cu nanoparticle and Cu@C composite, in general, and Cu@C, in particular, prove their potentiality for tribological applications.

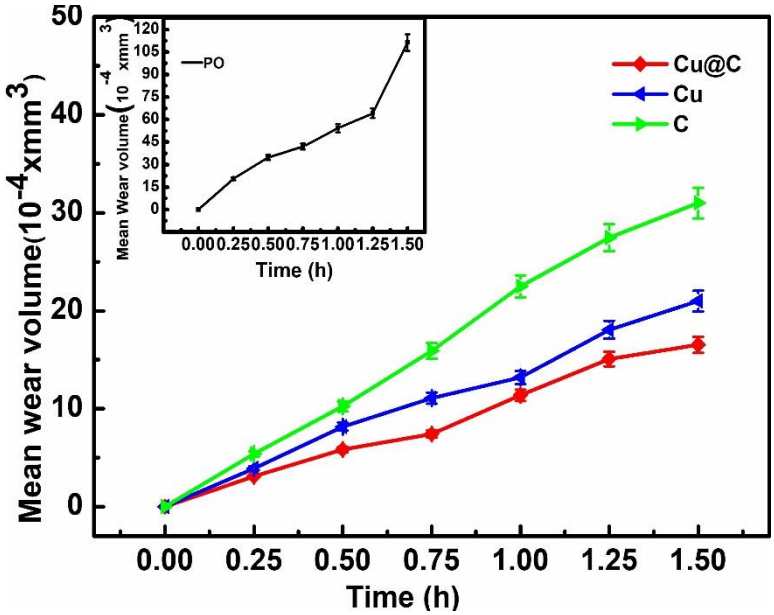

Fig. 5.10. Variation of mean wear volume of various additives with time at an optimum concentration of 0.1 % (w/v)

Table 5.1. Wear-rate for PO in the presence and absence of additive for 60 min test duration at 392 N applied load

S.N.	Lubricants	Wear rate (10^{-4} x mm^3/h)	
		Running-in	Steady-state
1	Cu@C	10.58	1.43
2	Cu	15.29	2.0
3	C	21.04	5.73

4	PO	69.99	38.88

5.2.2.4. Effect of load

For step loading test (ASTM D5183), at first wear test was run initially at 392 N load, 600 rpm, 75 ^{o}C temperature and 60 min. Time for the optimized concentration of additives assuming running-in period is over. The test was further continued for the steady-state by further stepwise addition of 98 N load after every 10 min, and corresponding frictional torque values were noted. The relevant data are displayed in **Fig. 5.11**. As per presupposition, the value of frictional torque is appreciably high in the presence of base lube, and seizure load is observed as 1078N. At seizure load, tribofilm undergoes depletion affecting the steady-state and lubricant turns incompatible with carrying the load. For blends of base oil with different additives, the frictional torque values are relatively stabilized with step loading of 98N and passage of time as compared to the blank base oil. Seizure load is observed at 2352, 2842 and 3430 N in the presence of carbon spheres, copper nanoparticles and the composite Cu@C respectively as additives. Thus, the best load carrying capacity is shown by Cu@C.

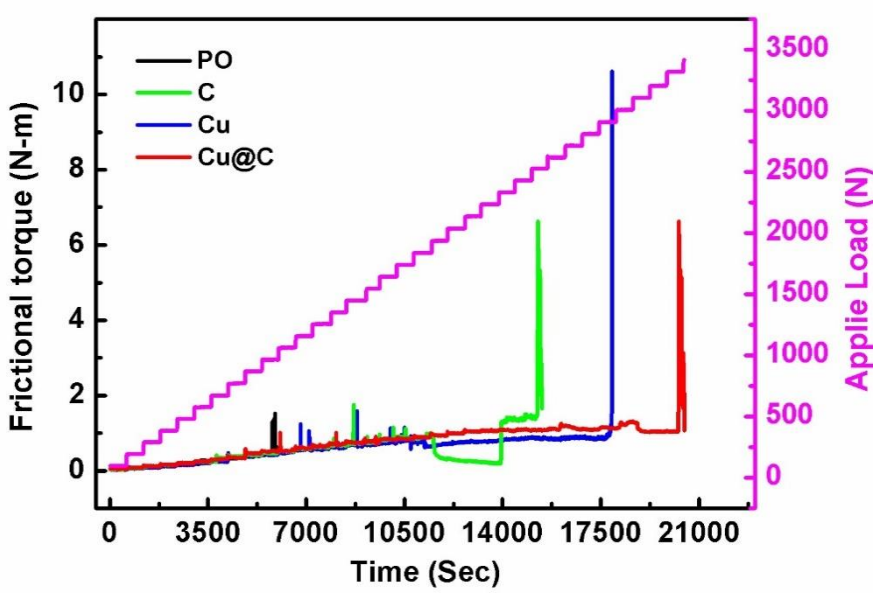

Fig. 5.11. Variation of frictional torque with time and step loading of 98 N after every 10 min of the test run for the optimized concentration of different additives

5.2.3. Surface Characterization

5.2.3.1. Surface morphology

The morphological features of the wear scar surface after ASTM D4172 test in the presence of base lube with and without additives have been examined by the surface techniques, AFM and SEM. The resulting SEM micrographs are illustrated in **Fig. 5.12**. In the presence of base oil alone, the surface seems to be abraded. Improvement of the surface in the presence of admixtures goes in the order of antiwear efficiency based on MWD, as shown in the micrographs. Accordingly, the minimum value of MWD and the smoothest wear scar surface lubricated with the blend of composite Cu@C support its candidacy for the potential triboactive additive.

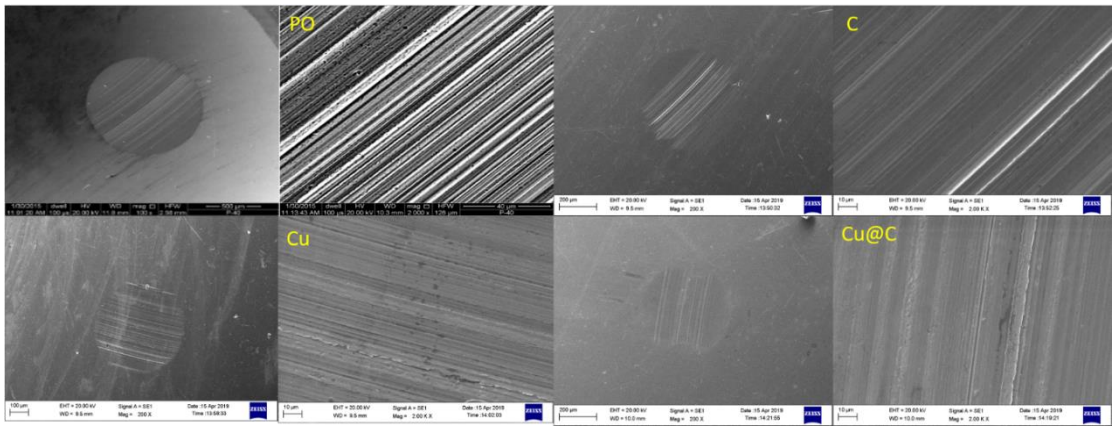

Fig. 5.12. SEM micrographs (Magnification 200 X and 2.00k X) of the worn surface of steel ball in the presence of base oil and its admixtures at 392 N load 60 min test duration

The smoothness of the surface in the presence of an admixture of additives was studied by contact mode AFM after the tribological tests at a 392 N load for 60 min duration. The roughness parameters of the wear scar of C, Cu nanoparticle and Cu@C are exhibited by AFM images in **Fig. 5.13a, b, c** respectively. The very high values of the area and line roughness are apparent from the figure for the base lube (D. Verma et al. 2019) alone whereas admixtures containing carbon spheres, Cu nanoparticles and Cu@C (Sq =41 nm; Rq =20 nm) cause a severe reduction in these values. **Fig. 5.13d** shows a line profile of the worn surfaces in the presence of the additives' blends with the base oil, measured in the transverse direction of sliding. The line profile indicates that the smoothness in case of Cu@C is superior to the other additives Carbon spheres and Cu nanoparticles.

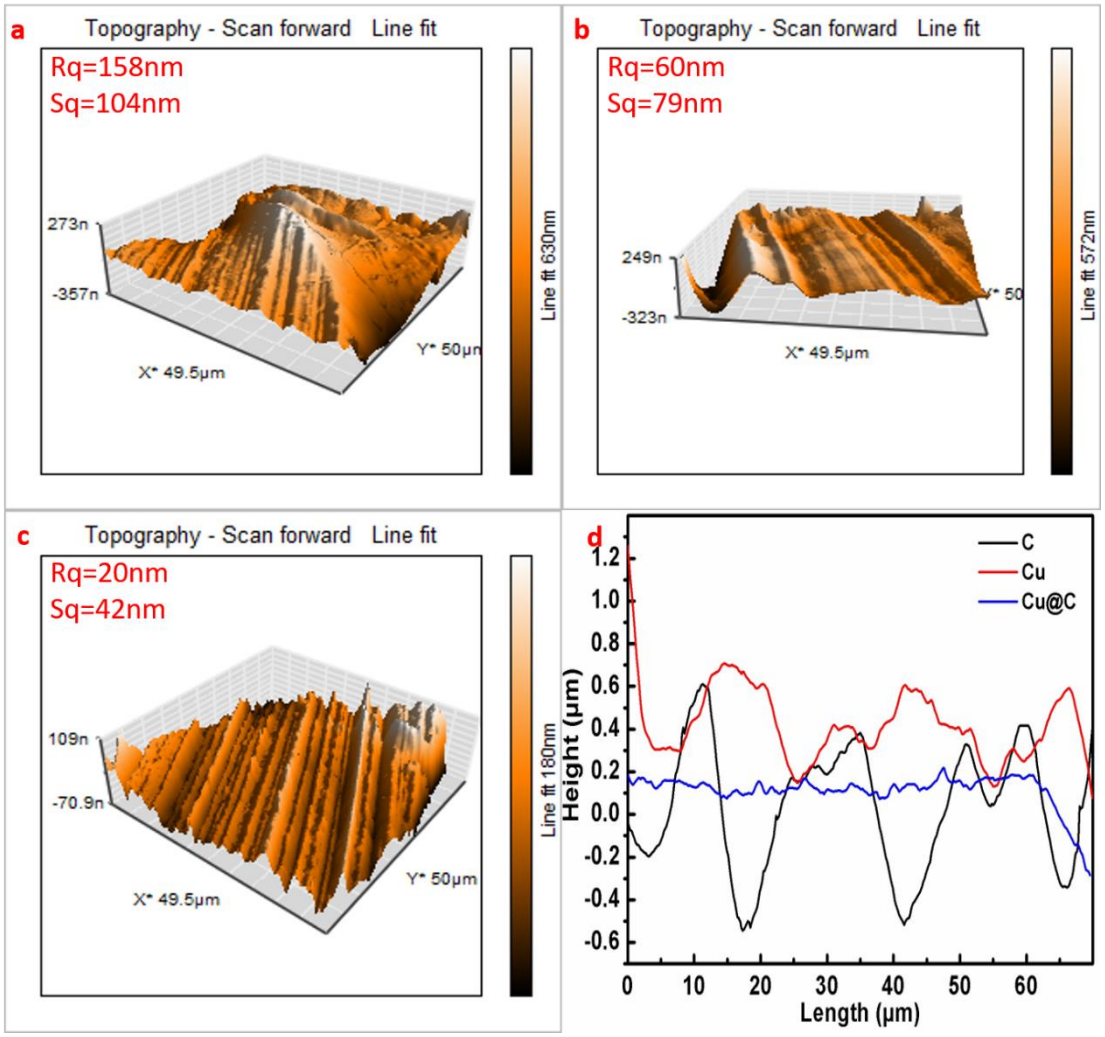

Fig. 5.13. *3D* AFM images of the worn steel surface lubricated with different additives in paraffin oil for 60 min test duration at a 392 N applied load (a) C, (b) Cu, (c) Cu@C and (d) line profile of worn surface of C, Cu and Cu@C

5.2.3.2. Tribochemistry

The EDX analysis of the worn surface in **Fig. 5.14** shows the presence of copper and carbon along with other elements providing evidence in favour of the active role played by the composite after adsorption on the surface.

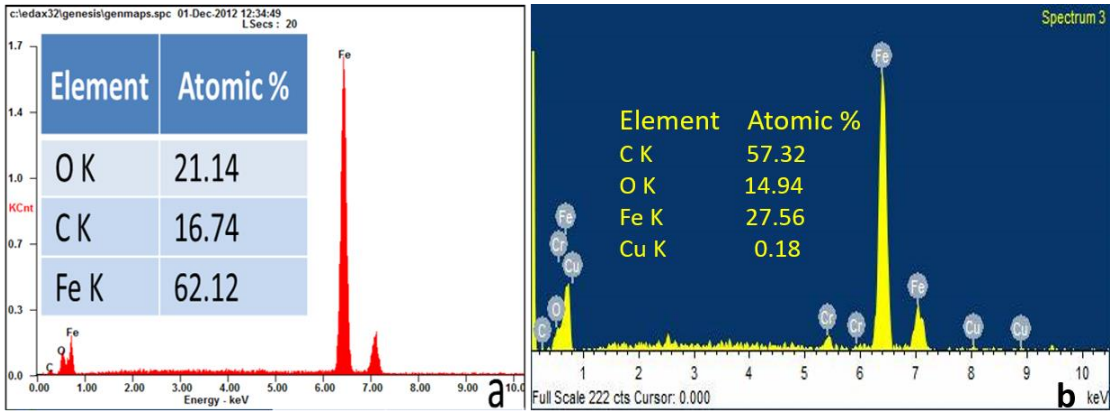

Fig. 5.14. EDX results for the worn surface of tested specimen balls lubricated with (a) paraffin oil (b) Cu@C

5.2.4. Mechanism of lubrication

Carbon spheres because of their completely spherical shape are supposed to slither along the surface and therefore improve lubrication between the interacting surfaces. At higher loads, carbon spheres may undergo deformation or even get smashed, resulting in the formation of debris, which may cause undue friction. The splendid tribological activity of the composite, Cu@C manifests the significant role of nanoparticles in enhancing the activity of carbon spheres. Copper nanoparticles have strengthened the carbonaceous tribofilm formed between the mating surfaces. The nanoparticles behaving as nano bearing facilitated the sliding motion. Their polishing effect assisted in the improvement of smoothness of the surface. Repairing of the surface through tribosinterzation of NPs also added to enhancement of surface smoothness of the tribo pairs as apparent from EDX spectra of the worn surface.

5.3. Conclusions

The copper nanoparticles, carbon spheres and the composite Cu@C have been prepared by hydrothermal method and characterized by techniques such as powder XRD, FE-SEM with EDX, TEM/HR-TEM, Raman and XPS spectroscopy. The dispersion stability of the new formulations in paraffin oil studied by electronic spectroscopy was found to be more than 48 hours. Tribo activity of the additives was assessed at 0.1% w/v concentration performing ASTM D4172 and ASTM D5183 tests on four-ball tribo tester. Based on the acquired data for mean wear scar diameter (MWD), coefficient of friction (COF), load-carrying capacity and wear rates, the efficacy of the additives to amend friction, wear and load-carrying capacity of the base lube could be established to fall in the order mentioned below:

Cu@C > Cu NPs > Carbon spheres > paraffin oil

The same order of activity is validated by studies related to surface characteristics by SEM and surface roughness data procured from AFM micrographs. The excellent activity of the nanocomposite appears to be a testament for strong reinforcement of carbon nanospheres by nanoparticles as ratified by the presence of copper along with carbon in EDX analysis of the wear scar. Thus, the composite Cu@C appears to be a prospective additive for reducing wear and friction.